Improvement of a Wavelet-Tensor Denoising Algorithm by Automatic Rank Estimation

Julien Marot(✉) and Salah Bourennane

Ecole Centrale Marseille, Institut Fresnel, Aix Marseille University,
D.U. de Saint Jérôme Av. escadrille Normandie-Niemen, 13397 Marseille, France
julien.marot@fresnel.fr

Abstract. This paper focuses on the denoising of multidimensional data by a tensor subspace-based method. In a seminal work, multiway Wiener filtering was developed to minimize the mean square error between an expected signal tensor and the estimated tensor. It was then placed in a wavelet framework. The reliable estimation of the subspace rank for each mode and wavelet decomposition level is still pending. For the first time in this paper, we aim at estimating the subspace ranks for all modes of the tensor data by minimizing a least squares criterion. To solve this problem, we adapt particle swarm optimization. An application involving an RGB image and hyperspectral images exemplifies our method: we compare the results obtained in terms of signal to noise ratio with a slice-by-slice ForWaRD denoising.

Keywords: MWF · Rank · PSO · Wavelets

1 Introduction

Hyperspectral images (HSI) are now currently used in remote sensing applications, for instance for aerial survey [1]. Most of HSIs, acquired by Hyperspectral Digital Imagery Collection Experiment (HYDICE) and Airborne Visible/ Infrared Imaging Spectrometer (AVIRIS) sensors, are impaired by noise from solar radiation, or atmospheric scattering [2]. Hence the interest of denoising HSIs, before applying further processings such as target detection.

Relation with Previous Work in the Field. A seminal work consisted in adapting Wiener filtering in a tensor framework, yielding the Multiway Wiener Filtering (MWF) [3], a subspace-based method requiring the estimation of ranks, usually performed with the statistical Akaike information criterion (AIC) [4], working best with a very high number of signal realizations. Recently, the MWPT-MWF (Multidimensional Wavelet Packet Transform-Multiway Wiener Filtering) method has been proposed [1,5], yielding good results in terms of signal to noise ratio (SNR) and classification accuracy. The drawback of this method is that a large number of subspace rank values must be estimated to ensure accurate denoising results. In [1], a study about the accurate depth of

S. Battiato et al. (Eds.): ACIVS 2015, LNCS 9386, pp. 779–790, 2015.
DOI: 10.1007/978-3-319-25903-1_67

the wavelet decomposition has been performed, but the subspace ranks are still estimated with AIC.

Goal and Contributions. In this paper, we propose a criterion and an optimization strategy based on particle swarm optimization (PSO) [6] to estimate the subspace ranks in MWF. We extend this strategy to the case where MWF is included in a wavelet framework. We infer from the large number of rank values to be thereby estimated that an accurate estimation has even more influence on the denoising quality.

Outline. Section 2 sets the problem of the subspace rank estimation in MWF and propose a criterion to minimize. In Section 3 we adapt PSO to rank estimation. In Section 4, we integrate rank estimation in a wavelet framework. In Section 5, the denoising results obtained with PSO or AIC are compared with truncation of HOSVD, MWF, or ForWaRD method [7].

2 Problem Setting

We consider a noisy multidimensional signal, also called tensor: a signal $\mathcal{X}$ impaired by a multidimensional additive white noise $\mathcal{N}$ [8]. The additive case generally holds for hyperspectral images [4,9]. As concerns the white noise assumption, it is also generally adopted for multidimensional images [8], and permits to focus on the main issue of this paper. In the case where the noise is not white, a prewhitening process could be applied as proposed in [10]. Thus, this tensor can be a model for an HSI, expressed as : $\mathcal{R} = \mathcal{X} + \mathcal{N}$. Tensors $\mathcal{R}$, $\mathcal{X}$, and $\mathcal{N}$ are of size $I_1 \times I_2 \times I_3$. For each spectral band indexed by $i = 1, \ldots, I_3$, the noise $\mathbf{N}(:,:,i)$ is assumed stationary zero-mean. We aim at denoising tensor $\mathcal{R}$ with a subspace-based method. Subspace-based methods have been shown to exhibit good denoising results when applied to data with salient main orientations in the image [11]. They provide an estimated signal tensor which, generally in the literature and in the remainder of this paper, is denoted by $\hat{\mathcal{X}}$. This estimate depends on the so-called 'subspace ranks' $\{K1, K2, K3\}$ which must be estimated. In the literature, the method which is proposed to estimate the subspace ranks is the AIC (Akaike Information Criterion) [8]. AIC estimates correctly the number of sources in an array processing problem. However, a large number of realizations of the same random signal are then available, hence the good behavior of AIC. Usually, in the frame of HSI processing, through a stationarity hypothesis, a covariance matrix is computed from the column vectors of the unfolded matrix obtained from the HSI, which are considered as realizations of the same random signal. AIC is applied to the eigenvalues of the covariance matrix obtained for each mode of the HSI [4]. However, it has been shown empirically that there is no clear domination of a subset of eigenvalues with high magnitude with respect to the others [4]. Hence, evaluating the best subspace ranks based on the eigenvalues only is not reliable. We propose to estimate the rank values through the minimization of a least squares criterion. MWF minimizes the MSE (mean square error) between expected and estimated tensor. So, we propose to minimize an MSE criterion to estimate the subspace ranks. It should increase the SNR values compared to an estimation with AIC. As a scalar criterion to estimate the subspace ranks $K1$, $K2$, $K3$, we choose:

$$J(K1, K2, K3) = ||\mathcal{R} - \hat{\mathcal{X}}||^2, \tag{1}$$

where $||.||$ represents the Frobenius norm. The criterion J is a nonlinear function of the parameters $K1, K2, K3$, hence the need for an adequate optimization method, which must be global.

3 Particle Swarm Optimization for Rank Estimation

Some global optimization methods may be available to minimize the criterion J of Eq. (1), but they exhibit some drawbacks: the DIRECT method [12], for instance, would assume J to be a Lipschitzian function of the ranks, which may not handle. The Nelder-Mead Simplex Method [13] is meant to minimize a scalar-valued nonlinear function of several real variables, without any derivative information. However, as specified in [13], the global convergence of the Nelder-Mead method is ensured only in a one-dimensional problem, and only if some conditions about the parameters involved in the method are respected. On the contrary, particle swarm optimization [6] provides the global minimum of a scalar function of several variables and is gradient-free. The basic PSO algorithm consists, for the current iteration number it, in computing the velocity:

$$\begin{aligned}\mathbf{v}_q^{K1,K2,K3}(\mathrm{it}+1) &= W\ \mathbf{v}_q^{K1,K2,K3}(\mathrm{it})...\\ ... &+ \gamma_{1q}\ r1_q(\mathbf{p}_q^{K1,K2,K3} - \mathbf{y}_q^{K1,K2,K3}(\mathrm{it}))\\ ... &+ \gamma_{2q}\ r2_q(\mathbf{G}^{K1,K2,K3} - \mathbf{y}_q^{K1,K2,K3}(\mathrm{it}))\end{aligned} \tag{2}$$

and the position:

$$\begin{aligned}\mathbf{y}_q^{K1,K2,K3}(\mathrm{it}+1) &= \mathbf{y}_q^{K1,K2,K3}(\mathrm{it})\\ ... &+ \mathbf{v}_q^{K1,K2,K3}(\mathrm{it}+1)\end{aligned} \tag{3}$$

In (2) and (3), $\mathbf{v}_q^{K1,K2,K3}(\mathrm{it})$ is the velocity of particle q at iteration it in a 3-dimensional space because there are 3 unknowns, W is the inertia weight, γ_{1q} and γ_{2q} are the acceleration constants encouraging a local and a global search respectively, $r1_q$ and $r2_q$ are random numbers between 0 and 1, applied to the q^{th} particle, $\mathbf{p}_q^{K1,K2,K3}$ is the best position found for particle q, $\mathbf{G}^{K1,K2,K3}$ is the best position found over the whole group, and $\mathbf{y}_q^{K1,K2,K3}(\mathrm{it})$ is the current position of particle q at iteration it. A large inertia weight (W) facilitates a global search while a small inertia weight facilitates a local search. We look forward to encourage a global search for the first iterations, and a local search for the last iterations. Hence, we fix an initial value W_{Init} and a final value W_{Final} for the weighting coefficient. At the iteration it, the weighting coefficient is computed as: $W = W_{Init} - \frac{(W_{Init}-W_{Final})*\mathrm{it}}{\mathrm{maxit}}$, where maxit is the final iteration number. When this last iteration number is attained, the position vector $\mathbf{y}^{K1,K2,K3}(\mathrm{maxit})$ contains the final estimated values $\hat{K1}, \hat{K2}, \hat{K3}$, of the signal subspace ranks.

4 Extension to the Wavelet Framework

We wish to adapt rank estimation to the most recent version of MWF, that is, its implementation in a wavelet framework [1]. This makes a reliable rank estimation method even more relevant: one triplet of rank values must be estimated for each wavelet coefficient. Following [1], minimizing the MSE between $\mathcal{X}$ and its estimate $\hat{\mathcal{X}}$ is equivalent to minimizing the MSE between $\mathcal{C}^{\mathcal{X}}_{\mathbf{l},\mathbf{m}}$ and $\hat{\mathcal{C}}^{\mathcal{X}}_{\mathbf{l},\mathbf{m}}$ for each $\mathbf{m}$:

$$\|\mathcal{X} - \hat{\mathcal{X}}\|^2 = \|\mathcal{C}^{\mathcal{X}}_{\mathbf{l}} - \hat{\mathcal{C}}^{\mathcal{X}}_{\mathbf{l}}\|^2 = \sum_{\mathbf{m}} \|\mathcal{C}^{\mathcal{X}}_{\mathbf{l},\mathbf{m}} - \hat{\mathcal{C}}^{\mathcal{X}}_{\mathbf{l},\mathbf{m}}\|^2 \tag{4}$$

where $\mathcal{C}^{\mathcal{X}}_{\mathbf{l}}$ is the wavelet packet coefficient tensor for levels in $\mathbf{l} = [l_1, l_2, l_3]^T$, $\mathcal{C}^{\mathcal{X}}_{\mathbf{l},\mathbf{m}}$ is the coefficient subtensor of $\mathcal{C}^{\mathcal{X}}_{\mathbf{l}}$ where $\mathbf{m} = [m_1, m_2, m_3]^T$ is the index vector, $1 \leq m_k \leq 2^{l_k} - 1$, $k = 1, \ldots, 3$.

We wish to minimize all terms of the summation in Eq. (4), knowing that the noise-free tensor $\mathcal{X}$ is not available. For this we propose Algorithm 1, *multidimensional wavelet packet transform and multiway Wiener filtering with rank estimation by particle swarm optimization* (MWPT-MWF-PSO). In Algorithm 1, $\mathbf{H}_{1,\mathbf{m}}, \mathbf{H}_{2,\mathbf{m}}, \mathbf{H}_{3,\mathbf{m}}$ denote the n-mode filters of MWF, which depend on rank values (K1,K2,K3) [1,8]; $\mathcal{C}^{\mathcal{R}}_{\mathbf{l},\mathbf{m}}$ denote the wavelet coefficients of $\mathcal{R}$.

Algorithm 1 MWPT-MWF-PSO

Input: noisy tensor $\mathcal{R}$.
• compute the wavelet decomposition of the noisy tensor $\mathcal{R}$: $\mathcal{C}^{\mathcal{R}}_{\mathbf{l}} = \mathcal{R} \times_1 \mathbf{W}_1 \times_2 \mathbf{W}_2 \times_3 \mathbf{W}_3$
• extract the wavelet coefficients [1]:
$\mathcal{C}^{\mathcal{R}}_{\mathbf{l},\mathbf{m}} = \mathcal{C}^{\mathcal{R}}_{\mathbf{l}} \times_1 \mathbf{E}_{m_1} \times_2 \mathbf{E}_{m_2} \times_3 \mathbf{E}_{m_3}$,
• for each wavelet coefficient $\mathcal{C}^{\mathcal{R}}_{\mathbf{l},\mathbf{m}}$:
i) estimate with PSO the optimal rank values $\hat{K1}, \hat{K2}, \hat{K3}$ in terms of the criterion:
$J_{\mathbf{m}}(K1, K2, K3) = ||\mathcal{C}^{\mathcal{R}}_{\mathbf{l},\mathbf{m}} - \hat{\mathcal{C}}^{\mathcal{X}}_{\mathbf{l},\mathbf{m}}||^2$
where $\hat{\mathcal{C}}^{\mathcal{X}}_{\mathbf{l},\mathbf{m}} = \mathcal{C}^{\mathcal{R}}_{\mathbf{l},\mathbf{m}} \times_1 \mathbf{H}_{1,\mathbf{m}} \times_2 \mathbf{H}_{2,\mathbf{m}} \times_3 \mathbf{H}_{3,\mathbf{m}}$.
As PSO is a global optimization method, algorithm 1 is supposed to converge asymptotically towards the best set of rank values. In practice, the total number of iterations, that is, the parameter maxit is fixed automatically: the algorithm stops when the criterion $J_{\mathbf{m}}(K1, K2, K3)$ does not vary from an iteration to another by a small factor ϵ set by the user.
ii) apply MWF to each coefficient subtensor $\mathcal{C}^{\mathcal{R}}_{\mathbf{l},\mathbf{m}}$, with the optimal rank values.
• obtain $\hat{\mathcal{C}}^{\mathcal{X}}_{\mathbf{l}}$ by concatenating all coefficients $\hat{\mathcal{C}}^{\mathcal{X}}_{\mathbf{l},\mathbf{m}}$.
• reconstruct the final estimated tensor by inverse wavelet transform: $\hat{\mathcal{X}} = \hat{\mathcal{C}}^{\mathcal{X}}_{\mathbf{l}} \times_1 \mathbf{W}_1^T \times_2 \mathbf{W}_2^T \times_3 \mathbf{W}_3^T$
Output: denoised tensor $\hat{\mathcal{X}}$.

5 Results

In this section, we apply the proposed method based on multiway Wiener filtering, multidimensional wavelet packet transform and particle swarm optimization, and comparative methods such as ForWaRD [7] on an RGB image and on real-world HSIs acquired by an AVIRIS sensor. ForWaRD is originally a deconvolution and denoising method. It includes first a Fourier Wiener filtering step and secondly a Wavelet filtering step. In the first step, a deconvolution process is proposed in the original paper [7]. In this paper, we avoid deconvolution as it is not required for the processed data, and use ForWaRD strictly as a denoising method. Programmes were written in $Matlab^{\circledR}$ language, and executed on a PC computer running Windows, with a 3GHz double core and 3GB RAM. The images are artificially impaired with white, identically distributed random noise. The denoising performance will be evaluated through SNR and $PSNR$: $SNR = 10\ log(\frac{||\mathcal{X}||^2}{||\mathcal{X}-\hat{\mathcal{X}}||^2})$ and $PSNR = 10\ log(\frac{||\max(\mathcal{X})||^2}{||\mathcal{X}-\hat{\mathcal{X}}||^2})$, where max denotes maximum value. The numerical results are computed from images truncated to the size $200 \times 200 \times 64$ to avoid the border issues. In the wavelet decomposition, following the recommendations in [1] we choose Coiflets and Daubechies wavelet functions. To choose adequately the number of decomposition levels for the considered noise level, we tested the two combinations proposed in [1]: either two or three decomposition levels for the space modes and no decomposition in the wavelength mode. Choosing $\mathbf{l} = [2, 2, 0]^T$, the results obtained with PSO are slightly better than with three decomposition levels, and those obtained with AIC hardly change. This yields 16 wavelet coefficients (4 coefficients for each level), which are 3^{rd}-order tensors of size $64 \times 64 \times 64$ for which the rank for each mode must be estimated. We initialize the ranks with a random value between 8 and 64. For this purpose we run the PSO algorithm with a swarm size 25 and a parameter $\epsilon = 10^{-6}$. This generally yields maxit = 150 iterations. The acceleration constants γ_{1i} and γ_{2i} are set to 2 and 3 respectively; the initial and final values of W are set to 0.9 and 0.4. ForWaRD is implemented with Daubechies wavelets, and two decomposition levels [7]. In the following subsections we present the numerical and visual results obtained with either ForWaRD algorithm [7], the truncation of HOSVD [8], or MWF [8] with the rank values which have been empirically found to yield the best results in terms of SNR; and MWF-MWPT in two configurations: the subspace ranks being estimated by AIC, and the subspace ranks being estimated with PSO (the proposed algorithm). As specified throughout the section, the input SNR is set to 10 dB for the first experiments, and then to 5, and 15 dB. For the RGB display of the hypespectral images throughout the section, we select 3 representative bands in the red, green, and blue wavelength domains respectively.

5.1 RGB Image

We apply denoising to the standard three-channel color image ‘Lena’ truncated to size 256×256. First, Table 1 provides the numerical results obtained when we impair the image in such a way that the input SNR is 10 dB. The original noise-free, noisy, and denoised images are displayed in Fig 1. Table 1 and Fig. 1

Table 1. SNR and PSNR values for the noised image; MWF with ranks fixed to 50, 50, 3; MWF of the multidimensional wavelet packet coefficients with rank estimation by AIC or by PSO (proposed method).

Method \ Criterion	SNR	PSNR
Noised image	10.00	20.20
MWF	14.17	19.06
MWF-MWPT:		
• AIC	14.85	19.75
• PSO	17.00	21.90

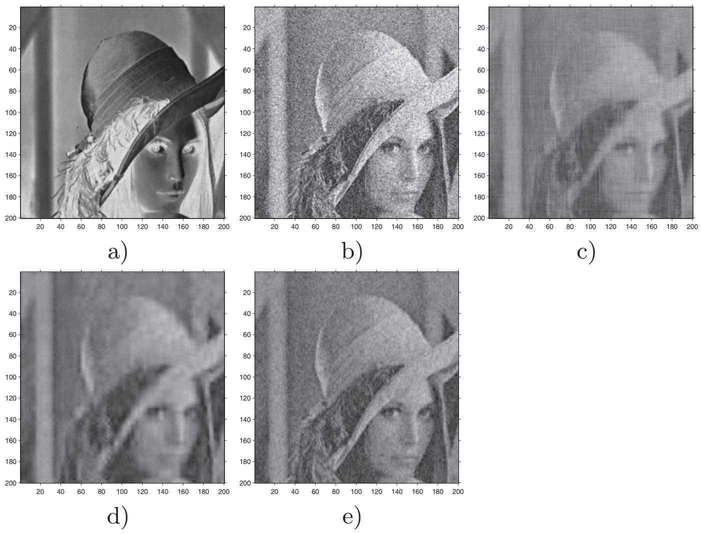

Fig. 1. a) Raw image; b) Noised image (10 dB); Denoising result: c) MWF, d) AIC, e) PSO.

show that the proposed method performs well on a color image, compared to MWF and the case where AIC criterion is used to estimate the ranks in a wavelet framework. Indeed for an input SNR of 10 dB the proposed method provides a denoised image with an output SNR of 17.00 dB, MWF provides 14.17 dB and AIC 14.85 dB. In the next two subsections, hyperspectral images are considered.

5.2 Hyperspectral Image AVIRIS 1

The HSI AVIRIS 1 is of size $256 \times 256 \times 64$, containing 64 wavelength channels. It contains rather straight orientations crossing the image. Hence, we expect that the original MWF, which applies a subspace-based filtering on the whole image, without wavelet decomposition, will provide rather good results. The ranks for the truncation of HOSVD and MWF are fixed to 50,50,20. The numerical results are provided in Table 2.

Table 2. AVIRIS 1: SNR and PSNR values for the noised image; Truncation of the HOSVD; MWF; MWF of the multidimensional wavelet packet coefficients with rank estimation by AIC or by PSO (proposed method).

Method \ Criterion	SNR	PSNR
Noised image	10.00	20.20
Truncation HOSVD	21.20	30.68
MWF	22.72	32.83
MWF-MWPT:		
• AIC	15.96	26.07
• PSO	21.30	31.41

When PSO is used, along the spatial modes, the ranks obtained for the approximation coefficients are between 20 and 64 (the maximum possible value), decreasing to 8 for the detail coefficients; along the wavelength mode, the rank is 8 (the smallest possible value). When AIC is used, along the spatial modes, the rank values vary from 1 to 64 without distinguishing between approximation and detail coefficients; along the wavelength mode, the rank values vary between 47 and 64, therefore much more elevated than in the case where PSO is used. Hence the lower noise magnitude in the case where PSO is used. Table 2 shows that, in the particular case of this image, MWF performs slightly better, in terms of SNR, than the proposed method. We notice however that estimating the rank values with PSO yields a better result than when AIC is used. However, the proposed method based on PSO provides the best visual result, as shown in Fig. 2 which presents the original noise-free (a), the noised (b), and denoised images for the comparative methods from c) to e) and the proposed method (f). Particularly, the contours are better preserved. See for instance the region between rows 120 to 140 and columns 30 to 80. A zoom on these regions is provided in Fig. 3. We infer from Fig. 3 that the proposed method better preserves the grey level values of each band in small regions.

The results obtained on the HSI AVIRIS 1 yields the following overall comments: when horizontal and vertical contours are present, there is no improvement -in terms of SNR- provided by the combination of wavelet decomposition and a subspace-based method such as MWF. However, the visual aspect is improved when the wavelet decomposition is performed. For the HSI AVIRIS

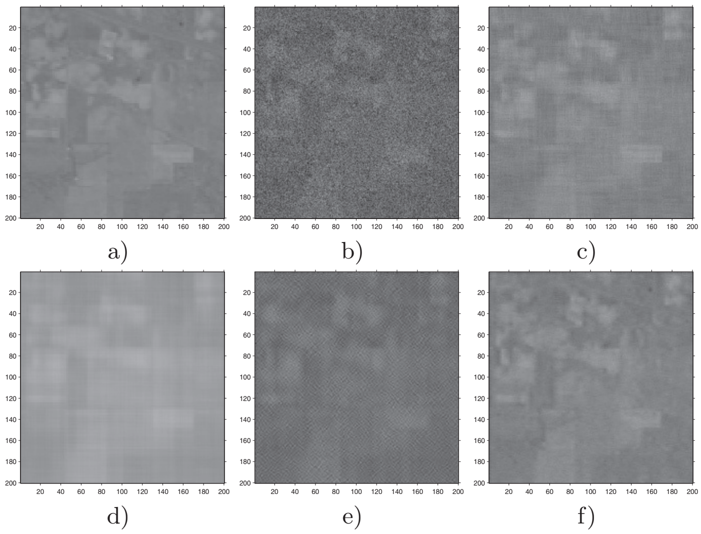

Fig. 2. AVIRIS 1: a) Raw image; b) Noised image (SNR 10 dB); Denoising result: c) Truncation of HOSVD, d) MWF, e) AIC, f) PSO.

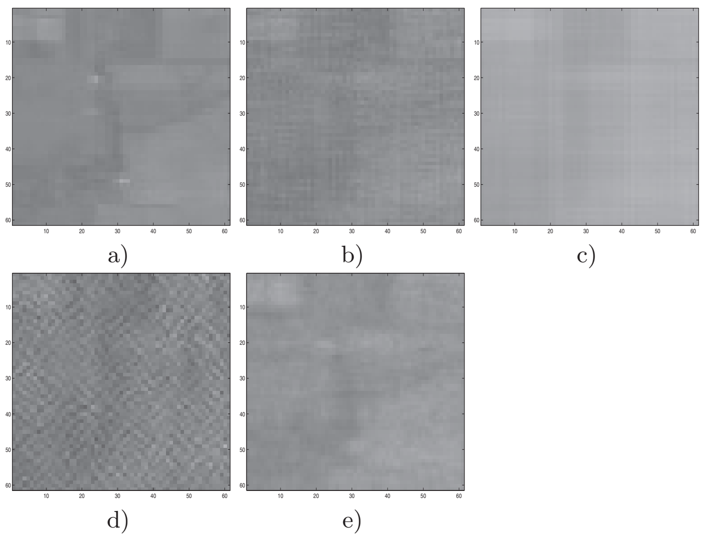

Fig. 3. Zoom on AVIRIS 1: a) Raw image, b) truncation of the HOSVD, c) MWF, d) AIC, e) PSO.

1, MWF takes advantage of the vertical and horizontal features present along the two spatial modes [8]. When small features are present instead, the interest of wavelet decomposition and of a correct subspace rank value in each mode will be emphasized.

5.3 Hyperspectral Image AVIRIS 2

In this subsection, we present results obtained on the HSI AVIRIS 2, of size $256 \times 256 \times 64$, where the relevant features are localized on some regions of the image. From the presence of such small local features we expect methods based on wavelet decomposition to provide better results compared to subspace-based methods, because wavelet decomposition permits to separate the processing of high frequency and low frequency features. We compare the results obtained with the wavelet-based ForWaRD algorithm [7] and MWF with ranks fixed to $50, 50, 20$.

Input SNR 10 dB: Numerical and Visual Results. First, we impair the image with an input SNR 10 dB. We obtain the numerical results (SNR and PSNR) presented in Table 3.

Table 3. AVIRIS 2: SNR and PSNR values for the noised image; comparative ForWaRD method; MWF; MWF of the multidimensional wavelet packet coefficients with rank estimation by AIC or by PSO (proposed method).

Method \ Criterion	SNR	PSNR
Noised image	10.00	23.13
ForWaRD	11.58	24.52
MWF	12.21	25.85
MWF-MWPT:		
• AIC	14.61	28.24
• PSO	18.58	32.21

Table 3 shows the superiority of the proposed method combining wavelet decomposition and rank estimation by PSO. The comparison with ForWaRD algorithm, which also works in the wavelet domain, shows that the proposed method is more appropriate to denoise such an HSI. Indeed, each spectral band is processed independently from the others with ForWaRD, whereas the tensor based methods using AIC or PSO take into account the relationships between bands. The original noise-free, noisy, and denoised images are displayed in Fig. 4. They show firstly that the result provided by MWF enhances some of the rows and columns which results in blurring the contours which are neither horizontal nor vertical. Also, they show that the homogeneous regions are better denoised with PSO than with AIC, or ForWaRD. In Fig. 5 we focus on the region containing the building and its frontiers (between rows 50 to 120 and columns 70 to 140 of AVIRIS 2). Comparing the result obtained by MWF and wavelet decomposition with rank estimation by PSO, we notice that the frontiers are much less blurred and that the details are better preserved when wavelet decomposition is used, and that the homogeneous regions are better denoised when PSO is used compared to the case where AIC is used. In this experiment, a close examination of the estimated rank values shows that, for the third mode, AIC tends to overestimate the ranks. We remind that the wavelet packet decomposition is performed with 2 levels on the two space modes, and that no decomposition is performed on the wavelength mode. When PSO is used, along the spatial modes, the rank values obtained are between 59 and 64; along the wavelength mode, the rank is always 8 (the smallest possible value). When AIC is used, along the spatial modes, the rank values vary from 2 to 64 with a much higher variability than in the case where PSO is used; along the wavelength mode, AIC yields elevated rank values between 51 and 64. PSO yields a stronger denoising in the wavelength mode and hence, overall, a better preservation of the spatial details and a higher output SNR.

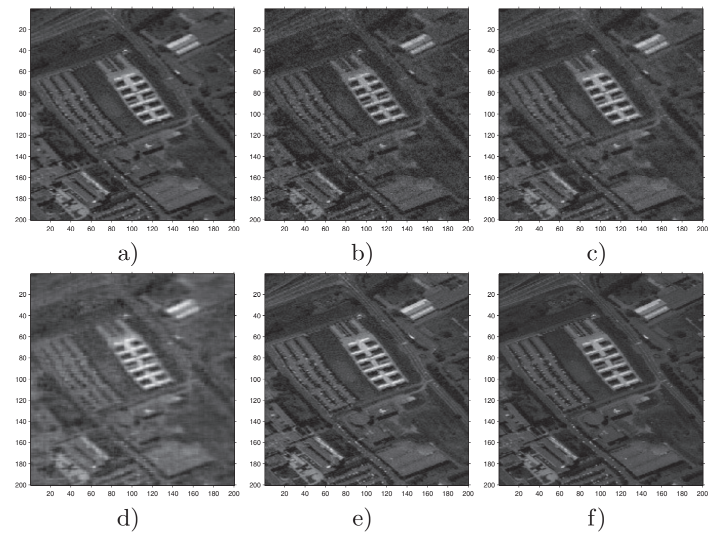

Fig. 4. AVIRIS 2: a) Raw image; b) Noised image (SNR 10 dB); Denoising result: c) ForWaRD, d) MWF, e) AIC, f) PSO.

The results obtained on AVIRIS 2 show the superiority of the proposed method not only in terms of image quality but also in terms of output SNR. To confirm this good behavior, we present, in the following, the results obtained on AVIRIS 2 with two other values of input SNR: 5 and 15 dB.

Input SNR 5 and 15 dB: Numerical Results. Here are some numerical results obtained with the image AVIRIS 2 and SNR=5 dB and SNR=15 dB in Table 4.

As a balance for the numerical results presented in Tables 3 and 4, we can assert that the rank values chosen by PSO yield the best denoising result in terms of SNR and PSNR at least when AVIRIS 2 is considered. We infer from these results that it is important to perform Wiener filtering in the wavelet domain,

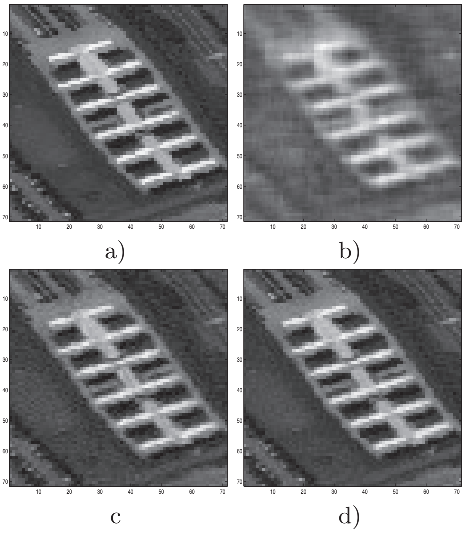

Fig. 5. Zoom on AVIRIS 2: a) Raw image, b) MWF, c) AIC, d) PSO.

Table 4. SNR and PSNR values for the noised image; comparative MWF; MWF-MWPT with rank estimation by AIC or by PSO (proposed method).

Criterion / Method	SNR	PSNR	SNR	PSNR
	5.00 dB		15.00 dB	
Noised image	5.00	19.22	15.00	28.73
MWF	10.61	24.23	12.99	26.62
MWF-MWPT:				
• AIC	11.17	24.79	18.98	32.60
• PSO	13.73	27.36	22.56	36.18

but also to use appropriate rank values to reach the best possible result in terms of SNR. This is the case as for AVIRIS 2 when the processed image contains small features such as buildings in aerial images, but also any small objects of interest. This appears very often in the case of other multidimensional images such as medical ones. Other experiments were performed with different images and SNR values. The corresponding numerical and visual results are provided at: `www.fresnel.fr/perso/marot/Documents/Resultsacivs.html`.

6 Conclusion

Recently, a common framework was proposed for multiway Wiener filtering and multidimensional wavelet decomposition, where a rank parameter must be available for each mode of the processed tensor, that is, 3 for an HSI, and for each decomposition level. This makes an automatic rank estimation method very valuable. AIC overestimates the expected values. We propose a novel approach which consists in minimizing a least squares criterion with particle swarm optimization, for each coefficient of the wavelet decomposition of the noisy tensor. Results obtained on an RGB image and noisy HSIs containing small features and details show the superiority of the proposed approach compared to AIC, FoRwaRD, HOSVD or MWF algorithms.

References

1. Lin, T., Bourennane, S.: Hyperspectral image processing by jointly filtering wavelet component tensor. IEEE Transactions on Geoscience and Remote Sensing **51**(6), 3529–3541 (2013)
2. Kerekes, J.P., Baum, J.E.: Full spectrum spectral imaging system analytical model. IEEE Trans. on Geosc. and Remote Sensing **43**(3), 571–580 (2005)
3. Muti, D., Bourennane, S.: Multidimensional filtering based on a tensor approach. Elsevier Signal Proceesing Journal **85**(12), 2338–2353 (2005)
4. Renard, N., Bourennane, S., Blanc-Talon, J.: Denoising and dimensionality reduction using multilinear tools for hyperspectral images. IEEE Geoscience and Remote Sensing Letters **5**(2), 138–142 (2008)
5. Lin, T., Marot, J., Bourennane, S.: Small target detection improvement in hyperspectral image. In: Blanc-Talon, J., Kasinski, A., Philips, W., Popescu, D., Scheunders, P. (eds.) ACIVS 2013. LNCS, vol. 8192, pp. 460–469. Springer, Heidelberg (2013)
6. Kennedy, J., Eberhart, R.: Particle swarm optimization. In: IEEE International Conference on Neural Networks, Perth, pp. 1942–1948 (1995)
7. Neelamani, R., Choi, H., Baraniuk, R.: Forward: Fourier-wavelet regularized deconvolution for ill-conditioned systems. IEEE Trans. on Signal Processing **52**(2), 418–433 (2004)
8. Muti, D., Bourennane, S., Marot, J.: Lower-rank tensor approximation and multiway filtering. SIAM Journal on Matrix Analysis and Applications **30**(3), 1172–1204 (2008)
9. Parra, L., Spence, C., Sajda, P., Ziehe, A., Müller, K.: Unmixing hyperspectral data. In: Advances in Neural Information Processing Systems, vol. 12, pp. 942–948 (2000)
10. Liu, X., Bourennane, S., Fossati, C.: Nonwhite Noise Reduction in Hyperspectral Images. IEEE Geoscience and Remote Sensing Letters **9**(3), 368–372 (2012)
11. Letexier, D., Bourennane, S., Blanc-Talon, J.: Main flattening directions and quadtree decomposition for multi-way wiener filtering. Signal, Image and Video Processing **1**(3), 253–256 (2007)
12. Jones, D.R., Pertunen, C.D., Stuckman, B.E.: Lipschitzian optimization without the lipschitz constant. Journal of Optimization Theory and Application **79**(1), 157–181 (1993)
13. Lagarias, J.C., Reeds, J.A., Wright, M.H., Wright, P.E.: Convergence properties of the nelder-mead simplex method in low dimensions. SIAM Journal of Optimization **9**(1), 112–147 (1998)